

# Intracellular RNA cleavage by the hairpin ribozyme

Attila A. Seyhan, Jillian Amaral and John M. Burke\*

Markey Center for Molecular Genetics, Department of Microbiology and Molecular Genetics, 306 Stafford Hall, The University of Vermont, Burlington, VT 05405, USA

Received April 20, 1998; Revised and Accepted June 18, 1998

## ABSTRACT

**Studies involving ribozyme-directed inactivation of targeted RNA molecules have met with mixed success, making clear the importance of methods to measure and optimize ribozyme activity within cells. The interpretation of biochemical assays for determining ribozyme activity in the cellular environment have been complicated by recent results indicating that hammerhead and hairpin ribozymes can cleave RNA following cellular lysis. Here, we report the results of experiments in which the catalytic activity of hairpin ribozymes is monitored following expression in mammalian cells, and in which post-lysis cleavage is rigorously excluded through a series of biochemical and genetic controls. Following transient transfection, self-processing transcripts containing active and inactive hairpin ribozymes together with cleavable and non-cleavable substrates were generated within the cytoplasm of mouse OST7-1 cells using T7 RNA polymerase. Unprocessed RNA and products of intracellular cleavage were detected and analyzed using a primer-extension assay. Ribozyme-containing transcripts accumulated to a level of  $4 \times 10^4$  copies per cell, and self-processing proceeded to an extent of >75% within cells. Cellular RNA processing was blocked by mutations within the ribozyme ( $G_8A$ ,  $G_{21}U$ ) or substrate ( $\Delta A_{-1}$ ) that, *in vitro*, eliminate cleavage without affecting substrate binding. In addition to self-processing activity, *trans*-cleavage reactions were supported by the ribozyme-containing product of the self-processing reaction, and by the ribozyme linked to the non-cleavable substrate analog. Ribozyme activity was present in extracts of cells expressing constructs with active ribozyme domains. These results provide direct biochemical evidence for the catalytic activity of the hairpin ribozyme in a cellular environment, and indicate that self-processing ribozyme transcripts may be well suited for cellular RNA-inactivation experiments.**

## INTRODUCTION

The development of *trans*-acting ribozymes for biochemical studies, together with the recognition that substrate recognition resulted from simple base-pairing rules, led to the concept of

using engineered ribozymes for targeted RNA inactivation within cells (1–9). Numerous potential cellular applications of ribozymes have been proposed, and most fall into three major categories. First, ribozymes may be useful tools for identifying the function of mammalian genes. To date, the tremendous advances in the rate of discovery of novel genes have greatly outstripped the capacity to assign function to their products. Second, ribozymes may potentially be used as therapeutic agents in controlling or preventing viral infections, for example in AIDS. Third, ribozymes may be useful in selectively reducing the expression of defective genes, or the inappropriate expression of normal genes, for example in cancer.

Ribozyme research has proceeded aggressively on two fronts: (i) fundamental biochemical studies of the structure and activity of ribozymes, and (ii) cellular applications of ribozyme technology. While great successes in the structure–activity studies have been achieved, progress in the cellular arena has, on the whole, been much slower. There are numerous possible reasons for relatively slow progress in cellular RNA targeting studies. Vector availability has limited expression studies, partly because mammalian expression vector technology has focused on the expression of mRNAs rather than small artificial RNAs like ribozymes. Delivery of exogenously synthesized ribozymes requires the development of synthetic methods to generate adequate quantities of stable ribozymes and methods to deliver them in an active form within cells. Very little is known about the subcellular localization of the ribozymes and their RNA targets, and few studies have examined the effects of endogenous RNA-binding proteins and the intracellular ionic environment on ribozyme activity. Finally, there is virtually no information available on the rates of formation of functional ribozyme–substrate complexes within cells, or on the selectivity of ribozymes in the cellular environment.

The detection of intracellular RNA cleavage products following ribozyme-catalyzed cleavage is a challenging task, in part because the cleavage products are believed to be rapidly degraded (10–13). Several reports have appeared in which RNA cleavage products purporting to result from intracellular cleavage activity of ribozymes have been observed (11–12, 14–17). However, recent studies using hammerhead and hairpin ribozymes have shown that cleavage did not occur within the cell but, instead, during the procedures for RNA isolation and preparation that follow cell lysis (18, 19, A.A.Seyhan and J.M.Burke, in preparation). Retrospective analysis of the earlier reports indicates that in most cases the possibility of post-lysis cleavage cannot be ruled out.

\*To whom correspondence should be addressed. Tel: +1 802 656 8503; Fax: +1 802 656 8749; Email: jburke@zoo.uvm.edu

To begin to address the gaps in our knowledge of ribozyme activity within cells, we have initiated studies designed to compare activity in cells and in the test tube, using rigorous controls and methods that allow us to compare *in vivo* and *in vitro* activity as directly as possible. Our first study of this type was genetic in nature, and showed that a two-base mutation in an anti-HIV hairpin ribozyme prevents substrate binding *in vitro*, and eliminates the antiviral effect of the ribozyme in HIV-infected cells (20).

Here, we present an initial analysis of the RNA cleavage activity of hairpin ribozymes in mammalian cells. Our strategy involved the synthesis and analysis of self-cleaving RNA molecules, and mutant derivatives, in the test tube and in the cytoplasm of mammalian cells. To ensure that the molecules studied *in vitro* and *in vivo* are as similar as possible, we have used T7 RNA polymerase *in vitro*, and a murine fibroblast line (OST7-1) that constitutively synthesizes T7 RNA polymerase and confines it to the cytoplasm (15,21). Our results show that the hairpin ribozyme has substantial self-cleavage activity in the mammalian cytoplasm, processing at least 75% of the self-cleaving transcripts. Controls show that both ribozyme mutations and substrate mutations that abolish cleavage *in vitro* eliminate the observed activity. Two independent methods were employed to demonstrate that all detectable RNA processing has occurred within the cells, rather than during the RNA isolation and primer extension steps following cellular lysis. Furthermore, we find that self-cleaving derivatives of the hairpin ribozyme have significant *trans*-cleavage activity, suggesting that such self-processing molecules may be very useful in targeted degradation of cellular RNA molecules.

## MATERIALS AND METHODS

### Synthesis of oligonucleotides, substrates and ribozymes

DNA oligonucleotides were synthesized using standard phosphoramidite chemistry on an Applied Biosystems 392 DNA/RNA synthesizer. Synthetic substrates were synthesized either as dephosphorylated RNA oligonucleotides or were transcribed from synthetic DNA templates as described (22), and then dephosphorylated with calf intestinal alkaline phosphatase. Ribozymes were transcribed from plasmid templates as described (23,24). All RNAs were purified using denaturing polyacrylamide gel electrophoresis in Tris-borate/EDTA buffer, eluted by diffusion, and precipitated with ethanol (23,25). For 5'-end-labeling, gel-purified RNA was first dephosphorylated with calf intestinal alkaline phosphatase (Boehringer Mannheim; 1 U phosphatase per 50 pmol of RNA) for 1 h at 50°C and subsequently phosphorylated with [ $\gamma$ -<sup>32</sup>P]ATP and T4 polynucleotide kinase (USB). Labeled RNAs were repurified using size-exclusion columns (Centri-Sep, Princeton Separations).

### Construction of self-processing ribozyme-substrate expression vectors

Plasmids encoding the normal self-processing RNA (denoted SC) and the RNA with an inactive substrate (denoted IS) have been described previously (26). The sequences flanking the self-cleaving hairpin ribozyme construct containing a T7 RNA polymerase promoter are 5'-AAGCTTTAATACGACTCACTA-TAGG-self-cleaving ribozyme-AGATctgtcactctagaggatc-3'. The T7 promoter sequence is indicated by bold upper case letters.

Transcription starts at the underlined G. The binding site for the primer used in the primer extension assay is indicated by lower case letters. Synthetic duplex DNA encoding the ribozyme, substrate and flanking sequences was cloned into the *Hind*III and *Sal*I sites of plasmid pUC19. An additional construct encoding an inactive ribozyme (G<sub>8</sub>A, G<sub>21</sub>U) was generated from the plasmid encoding the self-cleaving RNA, using PCR-based oligonucleotide-directed mutagenesis (Stratagene, USA). All plasmid sequences were confirmed by DNA sequence analysis.

### Transcription and *in vitro* RNA processing

RNA molecules were transcribed from 1  $\mu$ g *Eco*RI-linearized plasmid template or from 0.2  $\mu$ g PCR amplicons using T7 RNA polymerase. Transcription reactions contained 40 mM Tris-HCl (pH 8.0), 25 mM MgCl<sub>2</sub>, 5 mM DTT, 1 mM spermidine, 1 mM each of ATP, UTP and GTP, 0.1 mM CTP, 0.01% Triton X-100, 12.5 U pancreatic RNase inhibitor (Ambion, Inc.), 4  $\mu$ l (40  $\mu$ Ci) 10 mM [ $\alpha$ -<sup>32</sup>P]CTP (3000 Ci/mmol), 3  $\mu$ l T7 RNA polymerase (~200 U/ $\mu$ l) in a final volume of 20  $\mu$ l. Reactions were allowed to proceed at 37°C for 2 h. Transcription reactions were treated with 2 U of ribonuclease free DNase I (Ambion, Inc.) for 15 min at 37°C and inactivated by 1  $\mu$ l of 0.5 M EDTA. RNA was denatured at 90°C for 2 min and resolved by electrophoresis through 10% denaturing polyacrylamide-8 M urea gels, then visualized by UV shadowing and by a brief exposure to an autoradiographic film. A larger scale (100  $\mu$ l) transcription reaction for ribozyme RNAs was carried out in the same manner, except that  $\leq$ 10  $\mu$ Ci radioactive nucleotide was included in the reaction. Bands of ribozyme RNAs were excised and eluted overnight at 4°C in 500 mM ammonium acetate, 0.1% SDS and 0.1 mM EDTA. The eluates were recovered by filtration, extracted sequentially with phenol and chloroform-isoamyl alcohol, and then precipitated with ethanol. RNA pellets were washed with 70% ethanol, dried, resuspended in 10 mM Tris-HCl (pH 7.5) and 1 mM EDTA and quantified by measuring absorbance at 260 nm. Results were quantified using a Bio-Rad GS-525 molecular imager and Molecular Analyst 2.1 software. The extent of processing was expressed as the percent of both 3' and 5' cleavage products relative to the full length unprocessed product plus both cleavage products.

### *Trans*-cleavage reactions *in vitro*

Single-turnover cleavage reactions were performed under conditions of ribozyme excess (100 nM) over 5'-[ $\gamma$ -<sup>32</sup>P]ATP radiolabeled substrate (~1 nM; 27). Ribozyme and substrate were denatured separately for 2 min at 90°C in 50 mM Tris-HCl (pH 8.0) and 12 mM MgCl<sub>2</sub>, then renatured on ice for 30 min, and finally brought to 37°C for 10 min. Reactions were initiated by mixing an equal volume of ribozyme and substrate. Aliquots of the reaction (5  $\mu$ l) were removed, quenched with an equal volume of formamide loading buffer (90% formamide, 0.1% xylene cyanol, 0.1% bromophenol blue, 25 mM EDTA) and frozen at -20°C. Samples were denatured at 90°C for 2 min and separated on a 20% polyacrylamide-8 M urea gel. Results were quantified as described and plotted as the percent of the 5' cleavage product relative to the full length unprocessed RNA. The extent and the rate of cleavage were estimated by fitting the data to a single-exponential equation by non-linear regression analysis (27) using SigmaPlot 4.14 software (Jandel Scientific).

### Transient transfection of OST7-1 cells

One day prior to transfection, monolayers of mouse L9 fibroblast cell line OST7-1 (21) were seeded in 60 mm plates at a density of  $6 \times 10^5$  cells/plate in 3 ml of Dulbecco's modified Eagle's medium F-12 (Sigma) with 5% heat-inactivated (56°C, 30 min) fetal bovine serum and 2 mM L-glutamine (Sigma) containing 0.4 mg/ml of geneticin disulfate (G418; Sigma). Cells were grown overnight to 70–80% confluency. Transfections with plasmid DNA were performed using lipofectamine reagent (Gibco-BRL) in accordance with the manufacturer's instructions, as follows. Cells were transfected in duplicate with circular plasmids (1, 2 and 4 µg per plate) using 24 µl lipofectamine solution per plate. Briefly, appropriate quantities of each plasmid mixed with 300 µl of serum free Opti-MEM culture medium (Gibco-BRL), and 24 µl of lipofectamine reagent was mixed with 300 µl of Opti-MEM, representing duplicate independent transfections. The plasmid and lipid complex were combined and incubated at room temperature for 30 min to allow formation of the DNA–lipid complex. Cells were pre-washed twice with 2 ml of Opti-MEM, then overlaid with the DNA–lipid complex and incubated at 37°C in a 5% CO<sub>2</sub> incubator. After 5 h, the medium was replaced with 3 ml of fresh complete medium with serum, and then incubated for an additional 43 h.

### Extraction of total cellular RNA from OST7-1 cells

Total cellular RNAs were extracted essentially as described (28, as follows). Forty eight hours after transfection, cells were washed twice with 2 ml of 1 × PBS without Mg<sup>2+</sup> and Ca<sup>2+</sup>, then lysed by the addition of Trizol reagent [a monophasic solution of phenol, 4 M guanidinium isothiocyanate, 25 mM sodium citrate (pH 7.0) and 0.5% sarkosyl; Gibco-BRL]. The lysate was extracted once with 0.2 vol of chloroform, and the aqueous phase containing the total cellular RNA was precipitated with an equal volume of isopropyl alcohol. The resulting RNA pellet was washed with 75% ethanol, resuspended in water without further drying and quantified by spectrophotometric absorption at 260 nm.

### Primer extension analysis and RNA sequencing

Primer extension reactions were carried out basically as described (15,29). Two primers were used for primer extension. The first is complementary to the 3'-end of the self-cleaving ribozyme (5'-GATCCTCTAGAGTCGACAG-3'); it yields a 114 nt long extension product from full-length unprocessed RNA and a 32 nt long extension product from the 3'-cleavage product. The second primer is complementary to β-actin mRNA (5'-GAAG-GAGCTGCAAAGAAGCTGTG-3') and generates a 49 nt long primer extension band. Here, β-actin mRNA was used as an internal control to correct for variations in RNA yield and in gel loading. Purified cellular RNA (5 µg/reaction) was first denatured in the presence of [ $\gamma$ -<sup>32</sup>P]ATP-labeled DNA primers ( $4 \times 10^5$  d.p.m., ~50 fmol) by heating to 80°C for 10 min in 5 µl hybridization buffer [60 mM NaCl, 50 mM Tris-HCl (pH 7.5), 5 mM DDT] and then slowly cooled to 30°C for over 1 h to permit annealing of primers to their complementary RNAs. Annealed samples (2 µl) were then added to 3 µl of primer extension buffer (0.375 mM dNTPs, 1 × hybridization buffer). Sequencing ladders were generated by inclusion of 0.1 mM of the appropriate dideoxy ribonucleoside triphosphate. Reverse transcription reactions were initiated by adding MgCl<sub>2</sub> to 4 mM, or MnCl<sub>2</sub> to 1 mM, and 5 U of AMV

reverse transcriptase (USB) followed by a 30 min incubation at 47°C. Primer extension reactions were quenched by addition of an equal volume of formamide loading buffer containing 10 mM EDTA, denatured at 80°C for 2 min and then loaded on an 8% polyacrylamide–8 M urea sequencing gel. The extent of processing was expressed as the percent of 3'-cleavage product relative to the full length unprocessed product.

### Cleavage activity of expressed ribozymes *in vitro*

*In vitro* cleavage assays using ribozymes extracted from transiently transfected cells were performed as follows. Total cellular RNA (4 µg) from cells transfected with self-cleaving, inactive substrate and inactive ribozyme expression vectors (~0.3 nM) were pre-incubated at 90°C with 5' [ $\gamma$ -<sup>32</sup>P]ATP-labeled substrate (~3 nM) for 2 min in 50 mM Tris-HCl (pH 8.0) and 12 mM MgCl<sub>2</sub>, then incubated at 37°C under conditions of substrate excess. Aliquots for each time point (10 µl) were removed, quenched with equal volume of formamide loading buffer containing 25 mM EDTA and frozen at –20°C. Samples were denatured at 90°C for 2 min and cleavage products were separated from non-cleaved substrate by electrophoresis in 20% polyacrylamide–8 M urea gels.

## RESULTS

### Self-processing ribozyme cassettes and control constructs

We employed three versions of a DNA cassette encoding active and inactive self-cleaving hairpin ribozymes and substrates. These serve as templates for the transcription of RNA molecules comprised of substrates or non-cleavable substrate analogs linked to the 3' end of either active or inactive hairpin ribozymes (Fig. 1A and B). All ribozymes contained an extension of helix 4, previously shown to enhance catalytic activity (26). The normal self-cleaving construct (SC) consists of an active ribozyme linked to the normal substrate. The inactive substrate construct (IS) uses the active ribozyme with a substrate containing a deletion of A<sub>-1</sub>. The inactive ribozyme construct (IR) uses the normal substrate in conjunction with a ribozyme containing two point mutations, G<sub>8</sub>A and G<sub>21</sub>U. The IS and IR mutations were chosen because they eliminate cleavage, but do not inhibit formation of the ribozyme–substrate complex (30). The changes in the inactive substrate and inactive ribozyme constructs each completely eliminate self-cleavage of transcripts *in vitro* (Fig. 1C). Run-off transcription of the active construct undergoes very efficient self-cleavage *in vitro*, with a cleavage extent of ≥95% during transcription. The self-cleaving construct (SC) from a PCR template generates a minor (5%) 154 nt full-length product alongside 82 and 72 nt cleavage products, while the inactive substrate construct and inactive ribozyme construct showed no detectable reactivity (Fig. 1C).

### Trans-cleavage activity of self-processing ribozymes

We asked whether active or inactive self-processing transcripts were capable of supporting substrate cleavage reactions in *trans*. Each of the three constructs was used for *in vitro trans*-cleavage reactions under conditions of ribozyme excess, with a standard *trans*-ribozyme construct as control. To prevent annealing of ribozyme and substrate prior to the initiation of the reaction, the two RNAs were separately renatured and equilibrated in reaction buffer at 37°C prior to initiation of the reactions, which was

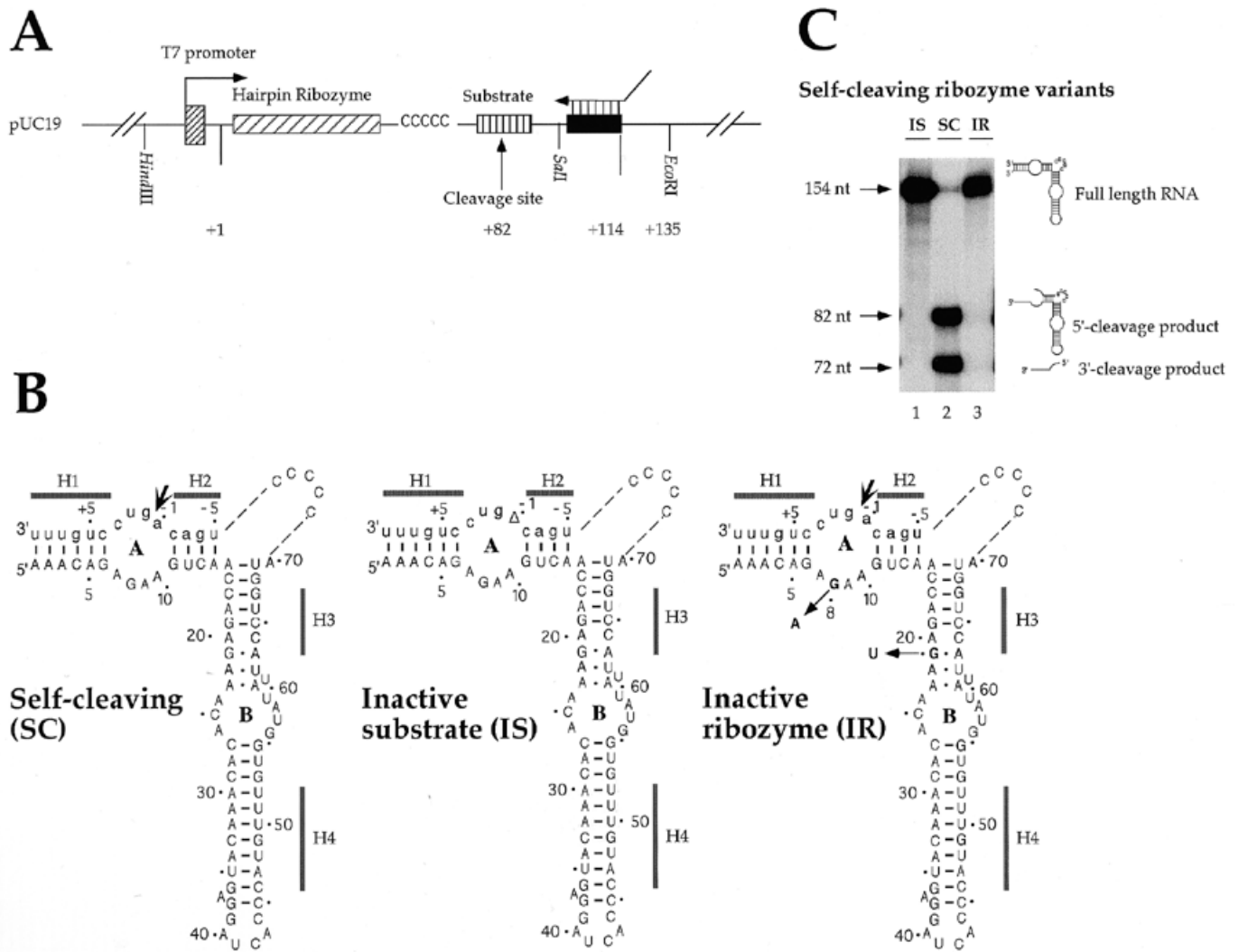


**Figure 1.** Transcriptional templates, ribozymes and *in vitro* RNA processing. (A) DNA encoding self-cleaving hairpin ribozyme construct. The ribozyme expression cassette depicted here was subcloned into the *Hind*III and *Sal*I sites of plasmid pUC19. The transcriptional initiation site and the direction of transcription are indicated with an arrow. Sequences encoding the ribozyme and cognate substrate are indicated as hatched rectangles. The primer-binding site for primer extension (solid rectangle) lies 32 nt downstream of the cleavage site. Run-off transcription from *Eco*RI-linearized templates generates a 135 nt full-length product, and ribozyme-catalyzed processing generates 82 and 53 nt 5' and 3' cleavage products, respectively. (B) Sequences and secondary structures of self-cleaving RNA molecules and mutant derivatives. The hairpin ribozyme is indicated by upper case letters; substrate is indicated by lower case letters. This construct is derived from the work of Feldstein and Bruening (42) with reinforcement of helix 4, previously shown to enhance catalytic activity (26). The four helical elements are indicated as H1–H4. The two internal loops are designated A and B. Non-canonical base pairs within loop B are as proposed by Butcher and Burke (23,29). Solid arrows indicate cleavage site. Bold letters with arrows indicate the sites of nucleotide substitution. The  $\Delta$  symbol indicates the site of nucleotide deletion. The binding sites of primers used in the primer extension assay lie to the 3' side of the sequences shown. (C) *In vitro* RNA processing activity of self-cleaving and mutant ribozyme constructs. Transcription reactions were carried out as described in Materials and Methods. Bands corresponding to the unprocessed ribozyme and the two cleavage products are indicated by schematic cartoon. Double-stranded DNA templates were generated by polymerase chain reaction using pUC/M13 forward (5'-TGTAACGACGGC-CAGT-3') and reverse primers (5'-CAGGAAACAGCTATGACC-3') from a plasmid template. Transcription reactions were separated on a 10% polyacrylamide–8 M urea gel, and gels were quantified using a Bio-Rad model GS-525 Molecular Imager and Molecular Analyst 2.1 software. The extent of processing is expressed as the percentage of 3' and 5' cleavage products relative to full length unprocessed RNA plus cleavage products. Run-off transcription of the self-cleaving construct (SC) from a PCR template generates a minor 154 nt full-length product alongside 82 and 72 nt cleavage products. The inactive substrate construct (lane 1) and inactive ribozyme construct (lane 3) showed no detectable reactivity.

achieved by mixing of the ribozyme-containing transcript with the RNA-substrate.

Substantial levels of *trans*-cleavage activity were observed for both of the constructs that contained an active ribozyme (Fig. 2A). Under these conditions, the processed self-cleaving ribozyme cleaves substrate in *trans* with a rate of  $0.28 \text{ min}^{-1}$ , compared to

$0.75 \text{ min}^{-1}$  for the normal *trans*-acting ribozyme under identical conditions (Fig. 2B). The inactive substrate construct cleaved substrate in *trans* at a reduced rate,  $0.06 \text{ min}^{-1}$  (Fig. 2B). In all cases, the extents of cleavage exceeded 90% after 120 min. As expected, no cleavage was observed for the transcript containing the inactive ribozyme (Fig. 2).

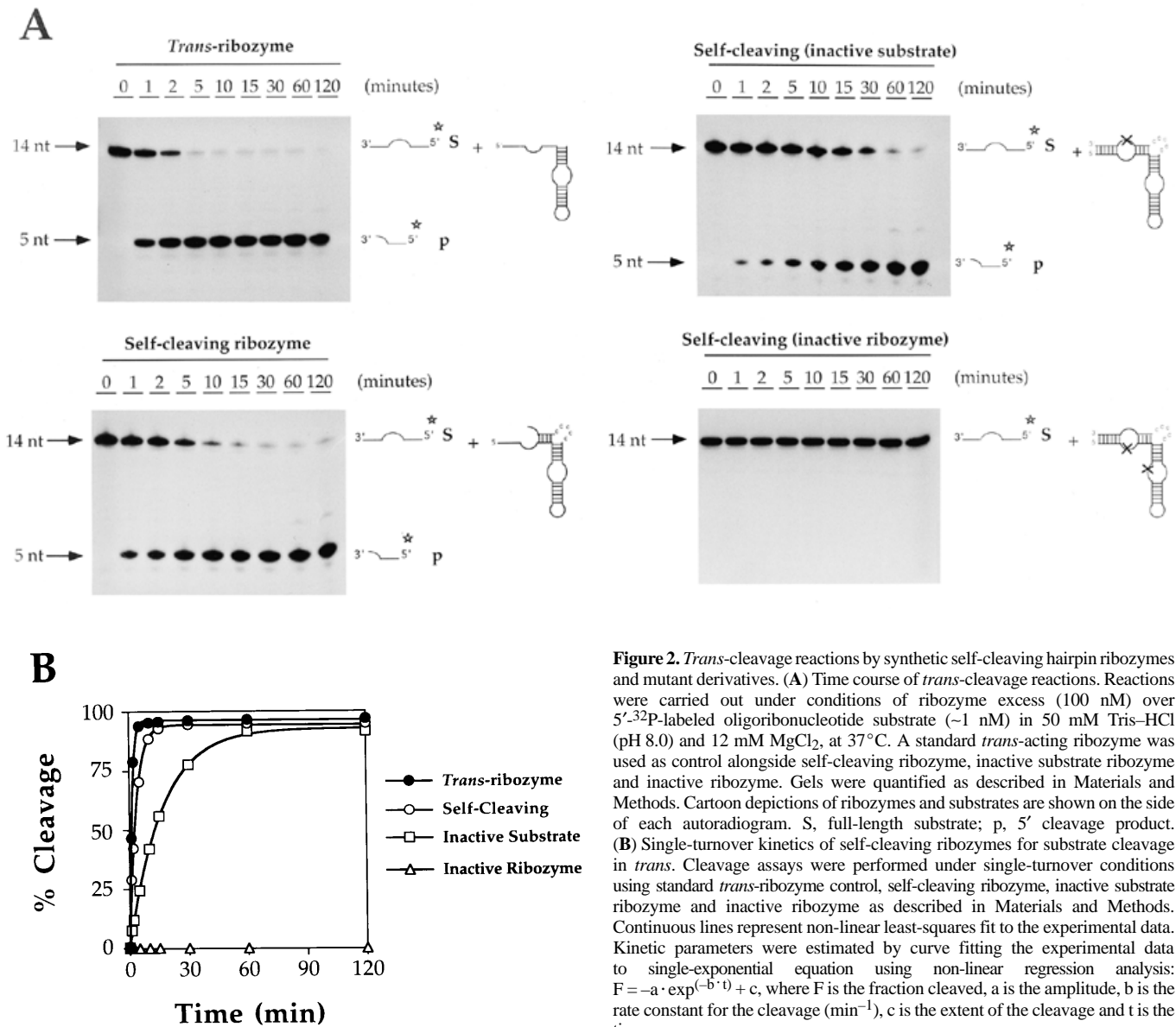


**Figure 2.** *Trans*-cleavage reactions by synthetic self-cleaving hairpin ribozymes and mutant derivatives. (A) Time course of *trans*-cleavage reactions. Reactions were carried out under conditions of ribozyme excess (100 nM) over 5'-<sup>32</sup>P-labeled oligoribonucleotide substrate (~1 nM) in 50 mM Tris-HCl (pH 8.0) and 12 mM MgCl<sub>2</sub>, at 37°C. A standard *trans*-acting ribozyme was used as control alongside self-cleaving ribozyme, inactive substrate ribozyme and inactive ribozyme. Gels were quantified as described in Materials and Methods. Cartoon depictions of ribozymes and substrates are shown on the side of each autoradiogram. S, full-length substrate; p, 5' cleavage product. (B) Single-turnover kinetics of self-cleaving ribozymes for substrate cleavage in *trans*. Cleavage assays were performed under single-turnover conditions using standard *trans*-ribozyme control, self-cleaving ribozyme, inactive substrate ribozyme and inactive ribozyme as described in Materials and Methods. Continuous lines represent non-linear least-squares fit to the experimental data. Kinetic parameters were estimated by curve fitting the experimental data to single-exponential equation using non-linear regression analysis:  $F = -a \cdot \exp(-b \cdot t) + c$ , where F is the fraction cleaved, a is the amplitude, b is the rate constant for the cleavage (min<sup>-1</sup>), c is the extent of the cleavage and t is the time.

### Ribozyme expression and processing in the cytoplasm of mammalian cells

Cytoplasmic RNA processing by hairpin ribozymes was investigated in OST7-1 cells using the identical constructs used for the *in vitro* studies described above. OST7-1 cells are murine L cells (fibroblasts) that constitutively express phage T7 RNA polymerase in the cytoplasm. Total cellular RNA was isolated 48 h following transient transfection. RNA was analyzed by primer extension analysis, using a radiolabeled 19 nt oligonucleotide primer that anneals downstream of the substrate cleavage site, and so is specific for both unprocessed transcripts and 3' processing products (Fig. 1A). A 23 nt primer complementary to a housekeeping gene,  $\beta$ -actin, was used as an RNA loading control. To identify bands, a dideoxy sequencing ladder was generated from the ribozyme-inactive substrate construct using the substrate-specific primer.

In cells transfected with each of the three plasmids, ribozyme-containing transcripts were readily detected using the primer-extension assay. Transcripts were not detected in control transfections in which either DNA or lipofectamine was omitted (Fig. 3A and see below).

Results for the cellular RNA processing reactions closely paralleled those obtained in simple buffers *in vitro*. For cells transfected with the plasmid encoding the self-cleaving RNA, the 32 nt fragment corresponding to the 3' cleavage product was the predominant species, and a relatively small proportion of uncleaved RNA was observed (Fig. 3A and see below). Alignment with the sequencing ladder confirms that the 5' end of the 3' cleavage product is G<sub>+1</sub>, as expected for hairpin ribozyme-catalyzed cleavage. If we assume that the 3' cleavage product and uncleaved RNA have the same stability in the cytoplasm (see Discussion), these results correspond to 75% ( $\pm 3\%$ ) self-cleavage within OST7-1 cells. No detectable cleavage was observed for the

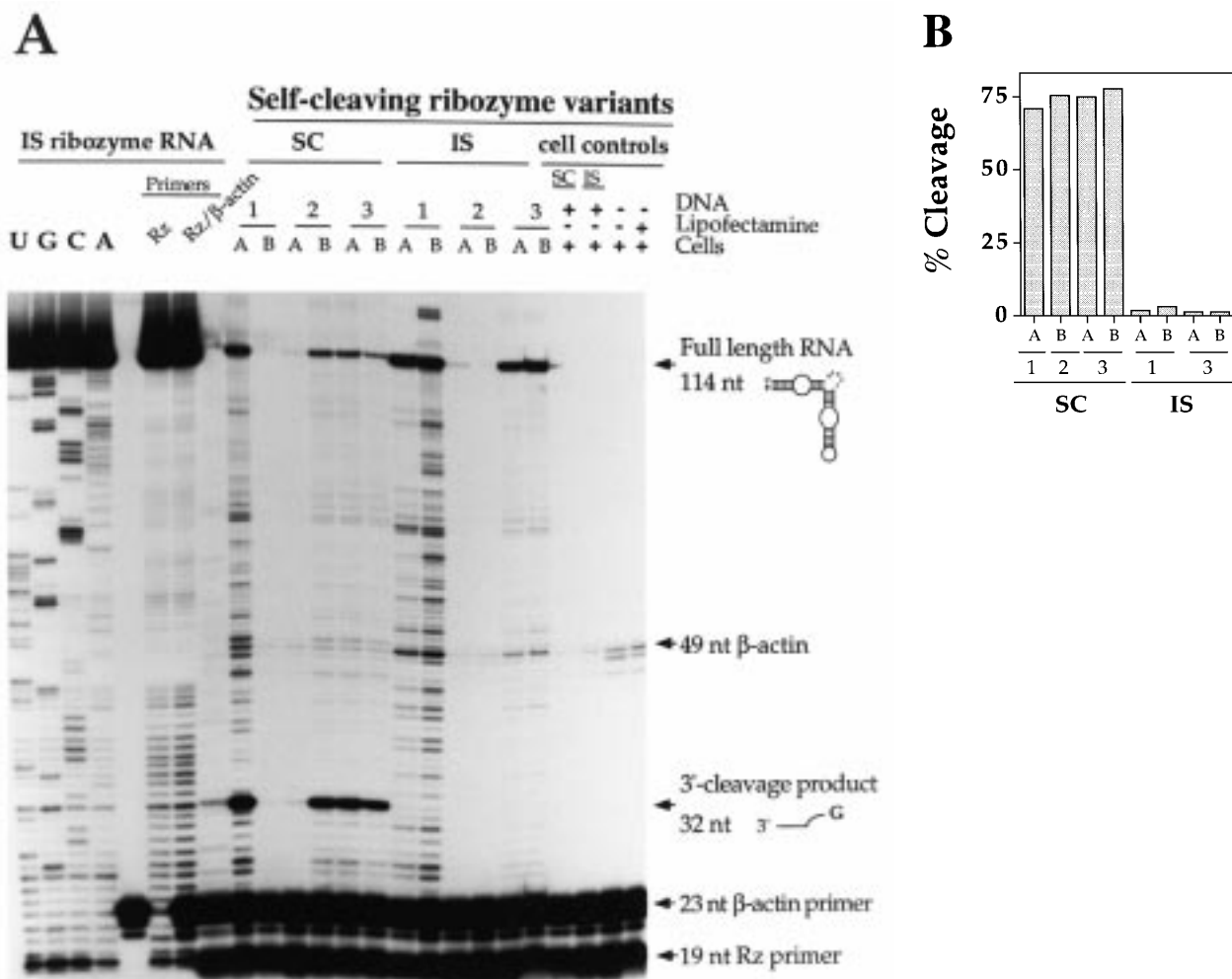


**Figure 3.** Expression and processing of RNA in the cytoplasm of mammalian cells. (A) Primer extension analysis of expression and processing. Primer extension assays were performed on unprocessed *in vitro* RNA transcripts of inactive substrate ribozyme, on total cellular RNA from cells transfected with self-cleaving and inactive substrate ribozymes, and on cellular RNA of untransfected cells, as described in Materials and Methods. Duplicate (A and B) independent transfections (1, 2 and 3) were performed, and RNA isolations and primer extension analysis were done as described in Materials and Methods. Cellular controls omitting lipofectamine, DNA or both, were included, as indicated. Arrows indicate the location of primer extension bands corresponding to full length RNA, 3' cleavage products,  $\beta$ -actin internal control gene and input primers. Sequencing ladders were generated as described in Materials and Methods. Primers, primer extension was performed on unprocessed *in vitro* RNA transcripts of inactive substrate ribozyme using ribozyme, and  $\beta$ -actin primers as a control for the assay, and primers. Rz, ribozyme; SC, self-cleaving ribozyme; IS, inactive substrate ribozyme. (B) Quantitation of RNA processing in OST7-1 cells. Results of primer extension analyses were quantified as described in Materials and Methods. The extent of processing is expressed as the percent of the 3' cleavage products band relative to the full length unprocessed RNA band. Duplicate transfections were assayed as described above. Note that four data points were not used in the graph due to lack of detectable signal [corresponding to lanes 1B and 2A of the SC set, and lanes 2A and 2B of the IS set in (A)].

ribozyme linked to the inactive ( $\leq 2\%$  self-cleavage in six replicate experiments) (Fig. 3). A separate primer extension assay was carried out on total cellular RNA from cells transfected with self-cleaving, inactive substrate, inactive ribozyme constructs, cellular RNA from untransfected cells, and unprocessed *in vitro* RNA transcripts of inactive substrate ribozyme. In this assay, 1 mM  $Mn^{2+}$  was used instead of 4 mM  $Mg^{2+}$  to prevent ribozyme catalysis during reverse transcription. Duplicate transfections were assayed as described previously.

The extent of intracellular self-processing by the self-cleaving ribozyme was 82% ( $\pm 1\%$ ) in OST7-1 cells (Fig. 4). The extent of the self-processing detected using  $Mn^{2+}$  in the primer extension assay closely paralleled those obtained using  $Mg^{2+}$  in the primer extension assay (Fig. 3). The two negative controls (inactive

ribozyme and inactive substrate) showed no evidence of RNA processing, although in each case the unprocessed transcript accumulated in substantial quantities (Fig. 4).

#### Intracellular accumulation of ribozyme-containing transcripts

A quantitative primer extension analysis was used to estimate the abundance of ribozyme-containing transcripts that accumulated within the cytoplasm of OST7-1 cells. Known amounts of unprocessed *in vitro* RNA transcripts of inactive substrate ribozyme (0.0004–400 fmol) were assayed by primer extension analysis alongside total cellular RNA from cells transfected with self-cleaving and inactive substrate ribozymes and cellular RNA of untransfected cells as described in Materials and Methods.

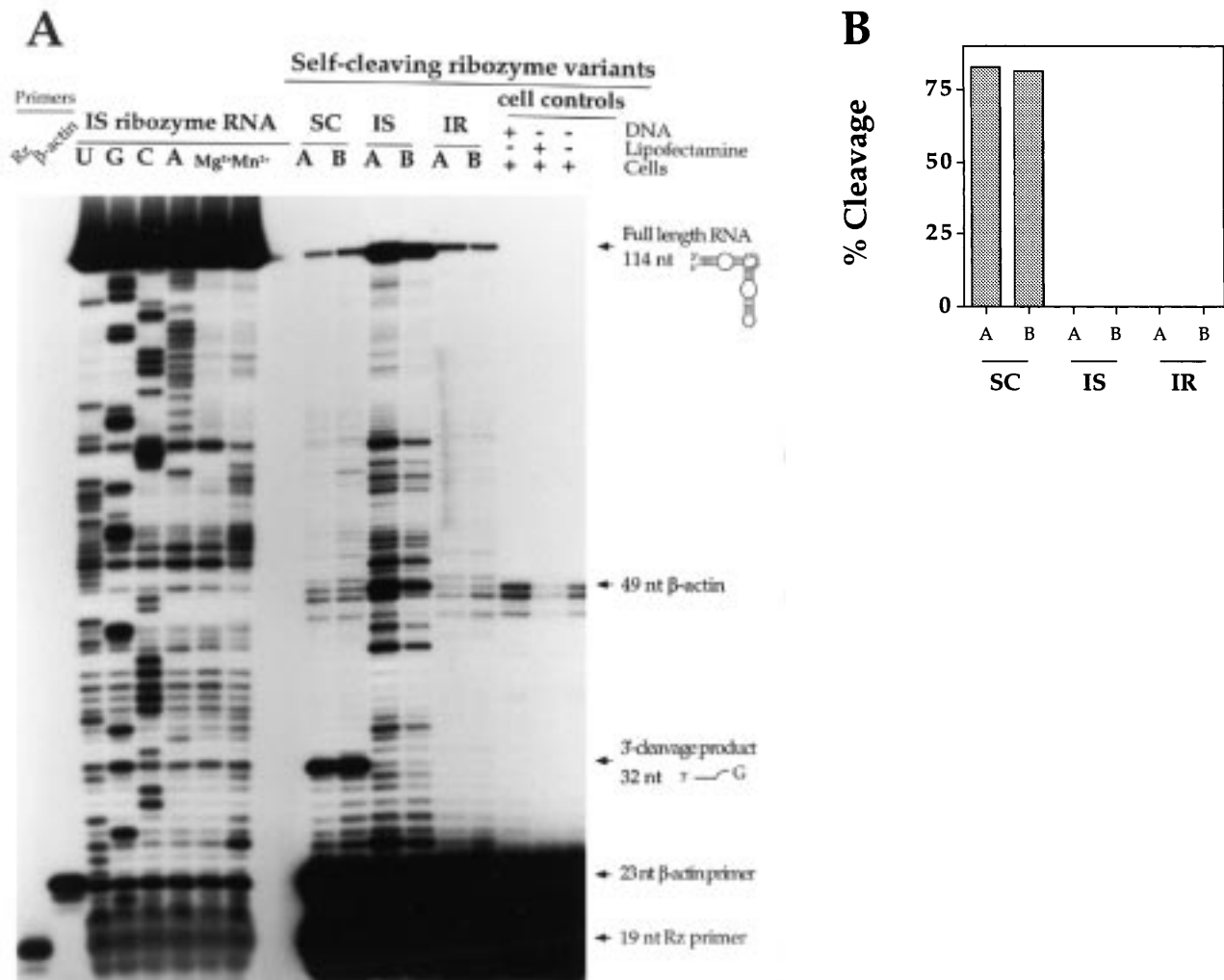


**Figure 4.** Primer extension analysis of cellular processing activity using  $Mn^{2+}$ . (A) Primer extension assays were performed on: (i) unprocessed *in vitro* RNA transcripts of inactive substrate ribozyme; (ii) total cellular RNA from cells transfected with self-cleaving, inactive substrate and inactive ribozyme constructs; and (iii) cellular RNA from untransfected cells. In the primer extension assay, 1 mM  $Mn^{2+}$  was used instead of 4 mM  $Mg^{2+}$ . Each transfection was done in duplicate, and independent primer extension assays were carried out on each RNA sample. As a control, primer extensions were performed on *in vitro* RNA transcripts using  $Mg^{2+}$  and  $Mn^{2+}$  respectively. Cellular controls omitting lipofectamine, DNA or both, were included, as indicated. Arrows indicate the location of primer extension bands corresponding to full length RNA, 3' cleavage products,  $\beta$ -actin internal control gene and input primers. Sequencing ladders were generated as described in Materials and Methods using 4 mM  $Mg^{2+}$ . Rz, ribozyme; SC, self-cleaving ribozyme; IS, inactive substrate ribozyme and IR, inactive ribozyme. (B) Quantitation of ribozyme processing in OST7-1 cells. The results were quantitated as described in Figure 3B and in Materials and Methods. Duplicate transfections were assayed as described previously.

Results were quantitated using a Bio-Rad GS-525 molecular imager and Molecular Analyst 2.1 software, and data were fitted using CA-Cricket Graph III, 1.5.1 software. A standard curve (31,32) was generated by quantitating the amount of full-length extension product obtained from quantities of an *in vitro* template. The amount of probe (~50 fmol) was always in large excess over the amount of target RNA used in the linear range of the standard curve (data not shown).

Two micrograms of total RNA (2  $\mu$ g per  $\sim 1 \times 10^5$  cells) were obtained from transfected cells, and used for primer extension analysis. Duplicate independent transfections were performed (Materials and Methods). Primer extension assays were carried out on each RNA sample. Calculations were based on an estimated RNA content of 26 pg per cell, and a cell volume of 4 pl, values determined using mouse L cells (31,33). The total RNA content per cell has been reported in the 10–30 pg range

(34,35). After correction for copy number per 26 pg total RNA (31), the number of molecules that remained undegraded by cellular ribonucleases was estimated per cell.

Results indicate a steady state level of ~44 000 molecules of ribozyme-containing transcripts per cell, at a time 48 h after the initiation of transfection. However, steady state level of ribozyme transcripts may vary among experiments depending on the state of the cells and the amount of DNA used.

#### **Trans-cleavage activity of expressed self-processing ribozymes in RNA extracts**

The activity of ribozymes expressed within OST7-1 cells was further confirmed by demonstrating that ribozyme activity is present in total cellular RNA extracts. For these experiments,  $^{32}P$ -labeled substrate was used under conditions of substrate

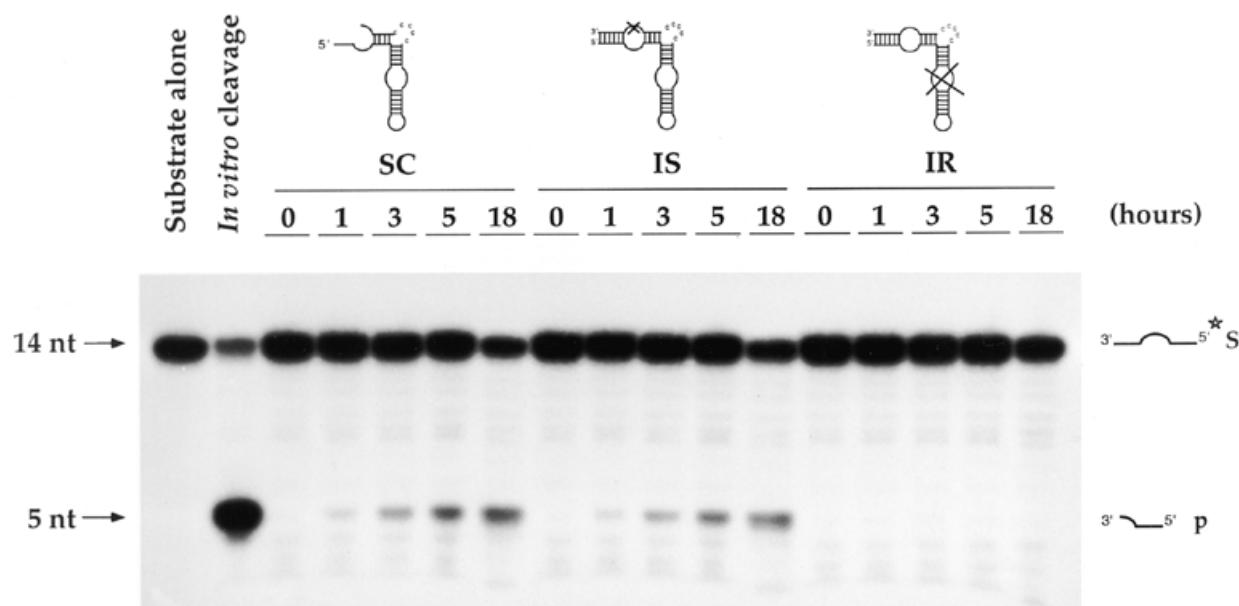


**Figure 5.** Ribozyme activity in total RNA extracts of OST7-1 cells. Self-cleaving ribozyme activity was assayed *in trans* in 4  $\mu$ g total RNA purified from transiently transfected cells expressing self-cleaving, inactive substrate and inactive ribozyme constructs. Cleavage reactions were carried out with end-labeled substrate ( $\sim 3$  nM) in excess over cellular ribozymes ( $\leq 0.3$  nM) in 50 mM Tris-HCl (pH 8.0) and 12 mM MgCl<sub>2</sub> at 37°C. Cartoon depiction of ribozymes and substrates are shown at the top of the autoradiogram. Extracts of cells expressing self-cleaving and inactive substrate ribozymes cleaved the substrate *in trans*. As expected, no cleavage was observed in extracts of cells expressing the inactive ribozyme. S, full length substrate; p, cleavage product; SC, self-cleaving ribozyme; IS, inactive substrate ribozyme and IR, inactive ribozyme.

excess. Cleavage activity was clearly detectable in total RNA extracted from cells expressing active ribozymes linked to either cleavable or non-cleavable substrates (Fig. 5). As expected, no cleavage was observed in RNA extracts of cells expressing the mutationally inactivated ribozyme. These results demonstrate that ribozyme molecules expressed within cells retain their structure and activity following the cell lysis and RNA extraction procedures, and that the ribozymes are able to bind and cleave substrate *in trans* in the highly complex environment of total cellular RNA.

#### RNA processing occurs within the cell, and not during RNA extraction, purification or primer extension

In two attempts to define the intracellular cleavage activity of hammerhead ribozymes, investigators found that the cleavage that they observed occurred not within the cells but, instead, took place during the RNA isolation procedure (18,19). We have recently found that both hairpin and hammerhead ribozymes can cleave their substrates if they are precipitated and dried, or are lyophilized, in the presence of monovalent cations, including those supplied in the form of Na<sub>2</sub>EDTA (A.A.Seyhan and J.M.Burke, in preparation). Therefore, we conducted an extensive series of experiments to determine whether the RNA cleavage that was observed occurred within the cell, or during one of the several steps that follow cell lysis, including RNA extraction, purification and primer extension.

To determine if cleavage could take place during the RNA isolation process, an excess of *trans*-acting ribozyme (10 nM), synthesized by *in vitro* transcription was pre-incubated at 37°C with 5' [ $\gamma$ -<sup>32</sup>P]ATP-labeled substrate ( $\sim 0.1$  nM) for 10 min in

water. Fluorescence quenching assays (36) demonstrate that complex formation does not occur in water alone (N.G.Walter and J.M.Burke, unpublished). Ribozyme and substrate RNAs were added to 1 ml cell lysate prepared as described above and then carried through the RNA extraction procedures. RNA extracted from this cell lysate was dissolved in 50  $\mu$ l of water. Aliquots with an appropriate specific activity were used for cleavage reactions at 37°C for 1 h with no added MgCl<sub>2</sub> and with 12 mM MgCl<sub>2</sub>. A third aliquot was carried through a mock primer extension assay without primers containing 0.375 mM dNTPs in 1  $\times$  hybridization buffer, 4 mM MgCl<sub>2</sub> and 5 U of AMV reverse transcriptase at 47°C for 30 min to examine ribozyme activity under these conditions. Reactions were stopped with an equal volume of formamide loading buffer containing 25 mM EDTA, denatured at 80°C for 2 min and separated by electrophoresis.

*Trans*-cleavage assays *in vitro* showed that the addition of cell lysis buffer, containing the denaturant guanidinium isothiocyanate, effectively inhibits hairpin ribozyme-catalyzed cleavage (data not shown). No cleavage was observed when we spiked the cell lysate with both *trans*-ribozyme and end-labeled substrate, and carried these RNAs through the RNA purification and primer extension protocols (Fig. 6A). However, when 12 mM Mg<sup>2+</sup> was added, a significant amount of the labeled substrate was cleaved. This indicates, first, that hairpin ribozyme-catalyzed cleavage activity can be obtained following cell lysis, if a suitable ionic environment is provided and, second, that the protocol that was used is sufficient to prevent cleavage from occurring after cellular lysis. Together, the results imply that the successful inhibition of cleavage results from the action of the denaturant and/or reduction of ionic concentration due to the approximately



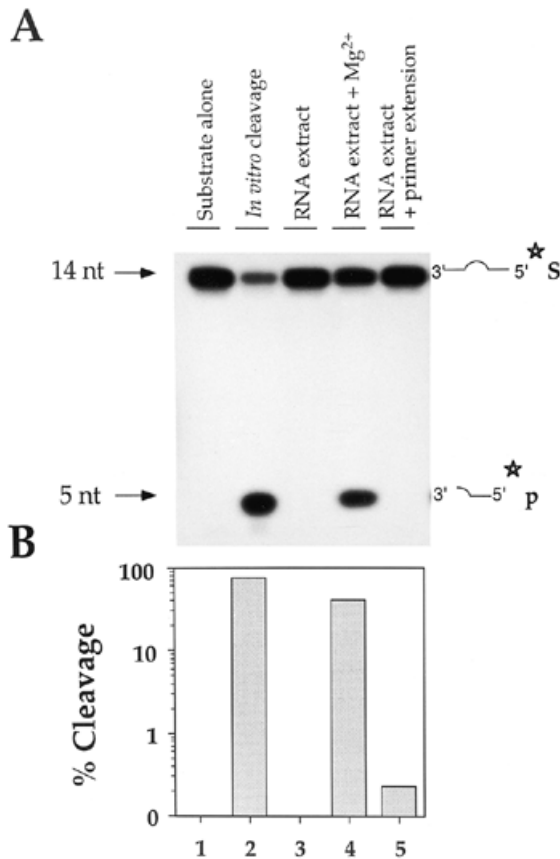


**Figure 6.** Ribozyme-catalyzed self-processing reactions do not occur during cell lysis, RNA purification or primer extension. (A) Autoradiogram of electrophoretic analysis. Post-lysis cleavage assays and mock primer extensions were performed on 1 ml of untransfected OST7-1 cell lysate as described in Materials and Methods. Single-turnover cleavage reactions were performed on oligoribonucleotide substrates. An excess of ribozyme (10 nM) was pre-incubated at 37°C with 5' [ $\gamma$ -<sup>32</sup>P]ATP-labeled oligoribonucleotide substrate (~0.1 nM) for 10 min. A solution containing ribozyme and substrate was then added to cell lysate, and carried through RNA extraction and purification in a manner exactly corresponding to that used for the intracellular activity assays. Substrate alone (lane 1) and a standard *in vitro* self-cleavage control (lane 2) were loaded alongside the post-lysis cleavage reaction mixes. Aliquots of purified RNA were loaded on a 20% denaturing polyacrylamide–8 M urea gel without further manipulation (lane 3). An aliquot was supplemented with 12 mM MgCl<sub>2</sub> and incubated at 37°C for 1 h (lane 4). For the mock primer extension assay (lane 5), the same quantity of RNA was carried through the primer extension protocol, but without primers, in the presence of 4 mM MgCl<sub>2</sub> as described in Materials and Methods. S, full-length substrate; p, cleavage product. (B) Quantitation of post-lysis ribozyme activity during RNA purification and primer extension. Cleavage reactions were performed as outlined above and in Materials and Methods. Results were quantitatively analyzed as described in Materials and Methods.

>200-fold dilution effect upon addition of a relatively large volume of lysis buffer to a small volume of cells.

To determine whether the conditions used for the primer-extension reactions would support RNA cleavage, we added the *trans*-ribozyme and labeled substrate to a primer extension reaction containing total cellular RNA extracts. This reaction contains 4 mM Mg<sup>2+</sup>, but the concentration of free magnesium is lower, due to chelation by deoxyribonucleoside triphosphates (total concentration, 0.75 mM). Under these conditions, cleavage

was greatly inhibited. Only ~0.25% of the labeled substrate was cleaved (Fig. 6), compared with a typical value of ≥95% cleavage under standard *in vitro* assay conditions. As a further control against cleavage during RNA isolation and primer extension, we replaced 4 mM Mg<sup>2+</sup> with 1 mM Mn<sup>2+</sup>. Manganese ions are known to support reverse transcriptase activity, but have been shown to significantly inhibit hairpin ribozymes with the wild-type substrate specificity (25 and data not shown); no hairpin ribozyme activity is observed in 1 mM Mn<sup>2+</sup>. Primer extension results obtained upon reverse transcription of cellular RNAs in the presence of Mn<sup>2+</sup> are congruent with those obtained in the experiments conducted with Mg<sup>2+</sup> (Figs 3 and 4). That is, the self-cleaving transcript processed to an extent of >80% while no cleavage of transcripts containing the inactive ribozyme or the inactive substrate was observed. Together, these experiments demonstrate that the conditions used for cell lysis, RNA isolation and primer extension do not support cleavage by hairpin ribozyme.

This series of control experiments strongly supports our conclusion that the appearance of RNA processing products derived from plasmid transcripts in OST7-1 cells results from intracellular catalysis by the hairpin ribozyme.

## DISCUSSION

Although a number of investigators have used ribozyme technology in work designed to selectively inhibit gene expression in cells, plants and animals, very little is known about the catalytic activity or selectivity of ribozymes within the complex cellular environment. The goal of the work described here is to begin to define the biochemical activity of hairpin ribozymes in a cellular setting, and to compare the intracellular activity of ribozymes to that observed in the test tube.

Our results clearly demonstrate that the hairpin ribozyme is active in the cytoplasm of OST7-1 cells, a fibroblast line that is a derivative of mouse L cells. In multiple experiments, we show that self-cleavage of a transcript containing a hairpin ribozyme and substrate takes place in such a manner that there is a large excess of 3' cleavage product over unprocessed RNA precursors at a time point 48 h after transfection.

Several lines of evidence indicate that formation of the cellular 3' cleavage product results from the catalytic activity of the ribozyme. First, the 5'-end of the 3' cleavage product corresponds to that predicted by analysis of the *in vitro* activity of the ribozyme. Second, the substrate mutation  $\Delta A_{-1}$  prevents self-cleavage *in vitro* and formation of the 3' cleavage product *in vivo*. Third, the ribozyme mutations G<sub>8</sub>A and G<sub>21</sub>U have the same inhibitory effects as the substrate mutation, both *in vitro* and *in vivo*.

Two independent experiments indicate that all, or essentially all, of the observed RNA cleavage took place within the cells prior to RNA extraction and purification. First, no cleavage of substrate occurred after adding exogenously synthesized ribozyme and labeled substrate to either the RNA extraction buffer or to the cell lysate containing the RNA extraction buffer. In contrast, cleavage was readily observed when the same mixture was supplemented with magnesium ions, indicating that the molecules are intact and capable of catalyzing the magnesium-dependent reaction. Second, no cleavage occurred when the primer extension assay was carried out in the presence of 1 mM Mn<sup>2+</sup> rather than 4 mM Mg<sup>2+</sup>. Previous work shows that replacing magnesium with manganese significantly inhibits the reaction (25), and that

essentially no self-cleavage is observed in 1 mM MnCl<sub>2</sub> (data not shown).

What do these experiments tell us about the relative catalytic activity of hairpin ribozymes in the test tube and in the mammalian cytoplasm? The apparent extent of self-cleavage in cells was ~80%, while the extent *in vitro* was higher, on the order of 95%. We believe that the 80% value may represent a lower limit for the actual extent of cleavage. Primer extension reactions are used to monitor the quantity of the 3' cleavage product following cleavage. Because the 3' cleavage product is short and unstructured, we believe that it is likely to be more rapidly degraded than the unprocessed precursor RNA by endogenous ribonuclease activities within the cells. If so, quantitating the 3' cleavage product would underestimate the actual extent of cleavage.

While we cannot assign a rate to the cytoplasmic self-cleavage reaction, the observation that self-cleavage proceeded nearly to completion is very encouraging for those engaged in the use of ribozymes for cellular RNA inactivation experiments. Based on our understanding of the requirements for the hairpin ribozyme reaction from *in vitro* studies, we would expect that the availability of magnesium ions within the cell might limit the reaction rate. While total intracellular magnesium concentrations as high as 10 mM have been reported, it has been estimated that the concentration of free magnesium ions available for use by the ribozyme is in the 1 mM range (37–39), well below the range that has been reported for high activity by the hairpin, hammerhead and other ribozymes. In this regard, it is possible that other inorganic cations, organic polyamines and RNA-binding proteins may act to reduce the intracellular magnesium requirement. Studies with HeLa cell nuclear and cytoplasmic extracts indicate that endogenous proteins moderately enhance the rate of the hairpin ribozyme cleavage reaction (Q.Yu and J.M.Burke, in preparation). If intracellular magnesium ion concentration is, in fact, limiting for *trans*-cleavage reactions, we will explore strategies to reduce the magnesium ion requirement, including *in vitro* selection (40).

Although numerous investigators have attempted to use ribozymes to inhibit gene expression, only a handful of studies have reported the direct observation of ribozyme activity, that is the formation of RNA cleavage products resulting from the putative catalytic action of ribozymes (11,12,14–17). Even in the cases where success has been reported, two recent studies indicate that it is possible or likely that the reported cleavage may actually have occurred not within the cell, but rather after the extraction of the RNA from the cells, during its workup for analysis (18,19). Therefore, we took all possible precautions to avoid post-lysis cleavage, and included several controls to detect post-lysis cleavage if it occurred. Based on the results of these experiments, we believe that we have rigorously demonstrated that essentially all of the substrate cleavage reported in our cellular studies has occurred within the cells.

Our finding that *in vitro* transcribed and expressed self-cleaving ribozymes can also cleave RNA in *trans* has important implications for targeted RNA cleavage. Expression of ribozyme-encoding sequences represents one important strategy for targeted RNA inactivation. Clearly, the presence of additional sequences appended to the ribozyme RNA has the probability of interfering with the catalytic activity of ribozymes, and the possibility of adversely affecting intracellular localization of the ribozyme-containing transcript. Self-processing transcripts have been proposed as a means to express multiple *trans*-acting ribozymes

from a single transcription unit (15,41). In these studies, additional self-processing cassettes were used to release the *trans*-acting ribozymes for targeted RNA cleavage. Our results indicate that these transcription units may be greatly simplified by using the same ribozymes for self-processing of the primary transcript and for targeted RNA cleavage.

We have shown that hairpin ribozymes have significant self-cleavage activity under the conditions that exist in the cytoplasm of mammalian cells. The use of transcripts containing mutations that eliminate catalytic activity of the ribozyme, together with a substrate mutation that prevents cleavage, provides strong evidence that the observed cleavage is catalyzed by the ribozyme and not by cellular ribonuclease activities. There are some limitations of this work. First, measurements of the extent of self-cleavage during a continuous transcription do not allow us to measure an intracellular cleavage rate. Second, we do not know the rates of endogenous degradation of the two cleavage products. However, enhanced degradation of the short, unstructured 3' cleavage product would artificially decrease the measured extent of cleavage.

Our results provide clear biochemical evidence supporting the use of hairpin ribozymes in RNA inactivation experiments in the cytoplasm. Work is currently underway to address issues of relative activity in the nuclear and cytoplasmic compartments, and to rigorously demonstrate *trans*-cleavage of targeted RNAs by engineered ribozymes in mammalian cells.

## ACKNOWLEDGEMENTS

We thank David Pecchia for gift of plasmids and synthesis of oligonucleotides, Jose Esteban for a gift of RNA, Nils Walter for the fluorescence assay and Jose Esteban, Joyce Heckman, Michele Shields, Nils Walter and Kyle O'Connor for helpful discussions. This work was supported by grants from the National Institutes of Health.

## REFERENCES

- Cech,T.R., Zaug,A.J. and Grabowski,P.J. (1981) *Cell*, **27**, 487–496.
- Zaug,A.J., Been,M.D. and Cech,T.R. (1986) *Nature*, **324**, 429–433.
- Prody,G.A., Bakos,J.T., Buzayan,J.M., Schneider,I.R. and Bruening,G. (1986) *Science*, **321**, 1577–1580.
- Cech,T.R. (1988) *J. Am. Med. Assoc.*, **260**, 3030–3034.
- Haseloff,J. and Gerlach,W.L. (1988) *Nature*, **334**, 585–591.
- Hampel,A. and Tritz,R. (1989) *Biochemistry*, **28**, 4929–4933.
- Feldstein,P.A., Buzayan,J.M. and Bruening,G. (1989) *Gene*, **82**, 53–61.
- Perrotta,A.T. and Been,M.D. (1990) *Nucleic Acids Res.*, **18**, 6821–6827.
- Long,D.M. and Uhlenbeck,O.C. (1993) *FASEB J.*, **7**, 25–30.
- Sioud,M. and Drlica,K. (1991) *Proc. Natl Acad. Sci. USA*, **88**, 7303–7307.
- Sioud,M., Natvig,J.B. and F rre, . (1992) *J. Mol. Biol.*, **223**, 831–835.
- Sioud,M., Opstad,A., Zhao,J.-Q., Levitz,R., Benham,C. and Drlica,K. (1994) *Nucleic Acids Res.*, **22**, 5571–5575.
- Ohkawa,J., Koguma,T., Kohda,T. and Taira,K. (1995) *J. Biochem.*, **118**, 251–258.
- Saxena,S.K. and Ackerman,E.J. (1990) *J. Biol. Chem.*, **265**, 17106–17109.
- Chowrira,B.M., Pavco,P.A. and McSwiggen,J.A. (1994) *J. Biol. Chem.*, **269**, 25856–25864.
- Borneman,J., Tritz,R., Hampel,A. and Altschuler,M. (1995) *Gene*, **159**, 137–142.
- Donahue,C.P. and Fedor,M.J. (1997) *RNA*, **3**, 961–973.
- Beck,J. and Nassal,M. (1995) *Nucleic Acids Res.*, **23**, 4954–4962.
- Heidenreich,O., Xu,X. and Nerenberg,M. (1996) *Antisense Nucleic Acid Drug Dev.*, **6**, 141–144.
- Yamada,O., Kraus,G., Sargueil,B., Yu,Q., Burke,J.M. and Wong-Staal,F. (1996) *Virology*, **220**, 361–366.

- 21 Elroy-Stein,O. and Moss,B. (1990) *Proc. Natl Acad. Sci. USA*, **87**, 6743–6747.
- 22 Milligan,J.F. and Uhlenbeck,O.C. (1989) *Methods Enzymol.*, **180**, 51–62.
- 23 Butcher,S.E. and Burke,J.M. (1994) *Biochemistry*, **33**, 992–999.
- 24 Chowrira,B.M., Berzal-Herranz,A., Keller,C.F. and Burke,J.M. (1993) *J. Biol. Chem.*, **268**, 19458–19462.
- 25 Chowrira,B.M., Berzal-Herranz,A. and Burke,J.M. (1993) *Biochemistry*, **32**, 1088–1095.
- 26 Sargueil,B., Pecchia,D.B. and Burke,J.M. (1995) *Biochemistry*, **34**, 7739–7748.
- 27 Esteban,J., Banerjee,A.R. and Burke,J.M. (1997) *J. Biol. Chem.*, **272**, 13629–13639.
- 28 Chomczynski,P. and Sacchi,N. (1987) *Anal. Biochem.*, **162**, 156–159.
- 29 Butcher,S.E. and Burke,J.M. (1994) *J. Mol. Biol.*, **244**, 52–63.
- 30 Berzal-Herranz,A., Joseph,S., Chowrira,B.M., Butcher,S.E. and Burke,J.M. (1993) *EMBO J.*, **12**, 2567–2574.
- 31 Lee,J.J. and Costlow,N.A. (1987) *Methods Enzymol.*, **152**, 633–648.
- 32 Rymaszewski,Z., Abplanalp,W.A., Cohen,R.M. and Chomczynski,P. (1990) *Anal. Biochem.*, **188**, 91–96.
- 33 Bertrand,E., Pictet,R. and Grange,T. (1994) *Nucleic Acids Res.*, **22**, 293–300.
- 34 Thompson,J.D., Ayers,D.F., Malmstrom,T.A., McKenzie,T.L., Ganousis,L., Chowrira,B.M., Couture,L. and Stinchcomb,D.T. (1995) *Nucleic Acids Res.*, **23**, 2259–2268.
- 35 Sambrook,J., Fritsch,E.F. and Maniatis,T. (1989) *Molecular Cloning: A Laboratory Manual*, 2nd ed. Cold Spring Harbor Laboratory Press, Cold Spring Harbor, NY.
- 36 Walter,N. and Burke,J.M. (1997) *RNA*, **3**, 392–404.
- 37 London,R.E. (1991) *Annu. Rev. Physiol.*, **53**, 241–258.
- 38 Romani,A. and Scarpa,A. (1992) *Arch. Biochem. Biophys.*, **298**, 1–12.
- 39 Murphy,E. (1991) *Annu. Rev. Physiol.*, **53**, 273–287.
- 40 Berzal-Herranz,A., Joseph,S. and Burke,J.M. (1992) *Genes Dev.*, **6**, 129–134.
- 41 Ohkawa,J., Yuyama,N., Takebe,Y., Nishikawa,S. and Taira,K. (1993) *Proc. Natl Acad. Sci. USA*, **90**, 11302–11306.
- 42 Feldstein,P.A. and Bruening,G. (1993) *Nucleic Acids Res.*, **21**, 1991–1998.